DOI: 10.1002/ange.200803869

Sorption Enhancement

Enhancement of Sorption Processes in the Zeolite H-ZSM5 by Postsynthetic Surface Modification**

*Stephan J. Reitmeier, Oliver C. Gobin, Andreas Jentys, and Johannes A. Lercher**

Medium-pore-size zeolites such as H-ZSM5[1] are key catalyst components in many petrochemical and refining applications.[2–5] These molecular sieves are used not only in catalytic processes such as toluene alkylation,[6–9] disproportionation, and xylene isomerization,[5,10–13] but also for hydrocarbon separation.[14] Shape-selective sorption and transport[10,15,16] of (substituted) aromatic molecules are the key zeolites properties for these applications. Surface modification by chemical liquid deposition (CLD) and chemical vapor deposition (CVD), or modification of the outer surface and the pore apertures by precoking, has been used to fine tune these properties.[10,16] Recently, we experimentally differentiated the elementary steps during sorption of rigid molecules such as alkyl benzenes into the pores of the zeolite MFI. Using fast time-resolved infrared spectroscopy to monitor these transport and diffusion processes,[14,17] a complex, interconnected network of sequential transport steps has been established, as schematically depicted for benzene in Figure 1.[14] The derived model is able to coherently explain several unconnected theoretical[18–22] and experimental[23–29] studies focusing on sorption and diffusion[28,29] of aromatic molecules.

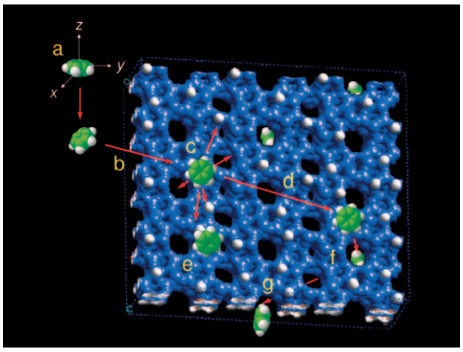

Figure 1. Schematic model describing the elementary transport steps from the gas phase with free molecular motion (a) to the active sites of H-ZSM5 during benzene sorption (adapted from reference [14]). A typical sketch of a H-ZSM5 crystal is shown with the zeolite lattice highlighted in blue and the hydrogen atoms in white. Preliminary collision with the zeolite surface (b), trapping in a weakly bound surface state (c), high surface mobility (d), parallel transport to the active sites (e) and in the pores (f), and finally intracrystal diffusion (g).

Overall, the macroscopic sorption process consists of five consecutive steps. These include collisions of gas-phase molecules with the external zeolite surface (Figure 1 b), the sorption into a physisorbed surface state characterized by high two-dimensional mobility (Figure 1 c), the parallel adsorption on terminal hydroxy groups (Figure 1 c,d), and the diffusion into the pores and subsequent sorption at intrapore sites (Figure 1 f).[10] Direct experimental evidence showed that the sticking probabilities for aromatic molecules on H-ZSM5 are unexpectedly small (on the order of 10^{-7}). Such low values are the consequence of the difference between the gas-phase and surface degrees of freedom in rigid molecules.[30] Primarily, the sticking of the aromatic molecules is governed by the sorbate mass and the decrease of entropy in the sorption process. The latter contribution is critically influenced by factors such as the geometrical sorbate dimensions, symmetry, and the space occupied on the surface as well as by the external morphology.[31] The observed order of the sticking probabilities on unmodified H-ZSM5 (*p*-xylene > benzene > *o*-xylene > toluene) agrees perfectly with the estimates by statistical thermodynamics, suggesting that overall, the sticking probabilities are strongly entropically controlled.[30,32]

Sorption of the relatively rigid aromatic molecules shows that the sticking probability is highly sensitive to the number of statistically favorable orientations of the molecules during the collision with the external surface.[31] Enhancing the total number of advantageous orientations of the molecules on the surface would lead to enhanced trapping of the molecules after the collision and as a direct consequence to markedly increased sticking probabilities. Using these results, it has been predicted that increased relative surface roughness, that is, a three-dimensionally structured surface induced by postsynthetic surface modification, enhances the number of advantageous orientations of symmetric molecules such as benzene in the sorption process, as it would allow them to retain a higher flexibility in their degrees of freedom when adsorbing from the gas phase.

With this background in mind, surface-modified H-ZSM5 zeolites were prepared as prototypes of a new series of zeolites that show enhanced sorption properties compared to conventional materials. Silica overlayers were prepared on H-ZSM5 (average particle size of 0.5 μm and Si/Al = 45:1), by reaction with tetraethylorthosilicate (TEOS) and subsequent hydrolysis and calcination. The unmodified sample is denoted

---

[*] S. J. Reitmeier, O. C. Gobin, Priv.-Doz. Dr. A. Jentys, Prof. J. A. Lercher
Technische Universität München
Lichtenbergstrasse 4, 85747 Garching (Germany)
Fax: (+49) 89-289-13544

[**] Financial support from the DFG under projects JE260-7/1 and JE260-8/1 is acknowledged. S.J.R. acknowledges the "Studienstiftung des Deutschen Volkes" for a PhD scholarship. We are grateful to Martin Neukamm, Dr. M. Hanzslik, and Prof. Dr. S. Weinkauf for the SEM and TEM measurements. We are also grateful for fruitful discussions in the framework of the center of excellence IDECAT and the graduate school NanoCat.

Supporting information for this article is available on the WWW under http://dx.doi.org/10.1002/anie.200803869.

H-ZSM5-p; the two TEOS-modified samples are called H-ZSM5-1m and H-ZSM5-3m, corresponding to one or three cycles of modification and calcination, respectively. The transmission electron micrographs of H-ZSM5-p show a clean, well-defined surface terminating the crystalline zeolite (Figure 2), suggesting a surface structure similar to that depicted in Figure 1. In contrast, the crystalline core of the modified material was (partially) surrounded by a thin and untextured region attributed to an amorphous SiO_2 layer (Figure 2). TEM images indicate the average thickness of the deposited layer to be 2.5–3.0 nm. Estimates based on the average crystallite size obtained by scanning electron microscopy (SEM) and the amount of TEOS added during the synthesis suggest an average thickness of approximately 3.0 nm. The statistically and randomly distributed deposits of SiO_2 on the zeolite generated by TEOS chemisorption, hydrolysis, and calcination led to a roughened external surface consisting of a porous amorphous overlayer. As a secondary effect, a minor fraction of the zeolite pores may be blocked or narrowed. Nitrogen physisorption (Table 1 and Figures S3 and S4 in the Supporting Information) was used to characterize the porosity of the amorphous layer.

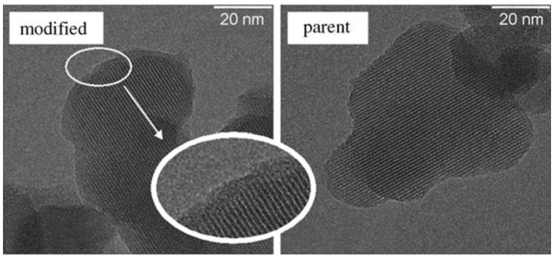

Figure 2. TEM images of typical H-ZSM5-p and modified H-ZSM5-3m samples in powder form. The inset emphasizes the partial fragments and overlayers of amorphous SiO_2 deposited on the surface. Combined with nitrogen physisorption measurements, the micrographs indicate an average thickness of the SiO_2 fragments of 2.5 to 3.0 nm. The fragments form large micropores of about 1.5 nm aperture.

Table 1: Selected structural properties of H-ZSM5-p and H-ZSM5-3 m.

Sample	S_{BET} [$m^2\,g^{-1}$]	V_{micro} [$cm^3\,g^{-1}$]	V_{meso} [$cm^3\,g^{-1}$]	V_{total} [$cm^3\,g^{-1}$]
H-ZSM5-p	423	0.121	0.017	0.364
H-ZSM5-3m	383	0.113	0.031	0.322
induced change	−40	−0.008	+0.014	−0.041

During modification, TEOS is hydrolyzed in the first step and condensed during the subsequent calcination steps, thus forming free hydroxy groups at the surface and in the pore mouth region, as described by Zheng et al.[35] A layer of SiO_2 consisting of large micropores (or small mesopores) is formed with an average porosity of approximately 30 %, calculated from the total amount of deposited SiO_2 combined with the N_2 physisorption. Especially the increase in mesopore volume ($+1.4\times10^{-2}\,cm^3\,g^{-1}$) of H-ZSM5-3m should be noted. Taken together, all characterization methods suggest that the H-ZSM5 crystals are partially covered by SiO_2 with an average thickness of 2.5–3.0 nm, which partially narrows the pore openings accidentally and forms large microporous channels with apertures of about 1.5 nm.

The individual sorption rates at the hydroxy groups on the outer surface and in the pores of the zeolite were studied by time-resolved rapid-scan IR spectroscopy. The coverage of the sorption sites was determined directly from the intensity changes of the bands using known molar absorbance coefficient. For H-ZSM5, the stretching vibrations located at 3745 and 3610 cm^{-1}, assigned to terminal and bridging hydroxy groups, were used to monitor the uptake of molecules on external and intrapore hydroxy groups. The molar extinction coefficients were determined from the concentration of these groups studied by ^1H MAS NMR (MAS = magic-angle spinning). The coverage changes during the rapid-scan experiment were fitted with an exponential function [see Eq. (1) and reference [30]] to calculate the initial sorption rates r_{ini}.

$$r_{ini} = k_{ad}\,\Delta c_{OH,eq}\,e^{-t/\tau_{ad}} \overset{t<\tau_{ad}}{\sim} k_{ad}\,\Delta c_{OH,eq} = \frac{\Delta c_{OH,eq}}{\tau_{ad}} \qquad (1)$$

Here, k_{ad} is the adsorption rate constant, $\Delta c_{OH,eq}$ is the change in equilibrium coverage of hydroxy groups, t is the scan time, and τ_{ad} is the time constant of adsorption. The characteristic time profiles of the coverage of the SiOH and SiOHAl groups are compiled in Figure 3, and the initial sorption rates are compared in Table 2.

Identical time constants were observed before and after modification for the terminal hydroxy groups, while the equilibrium coverage decreased after modification. This change is paralleled by the reduced concentration of the

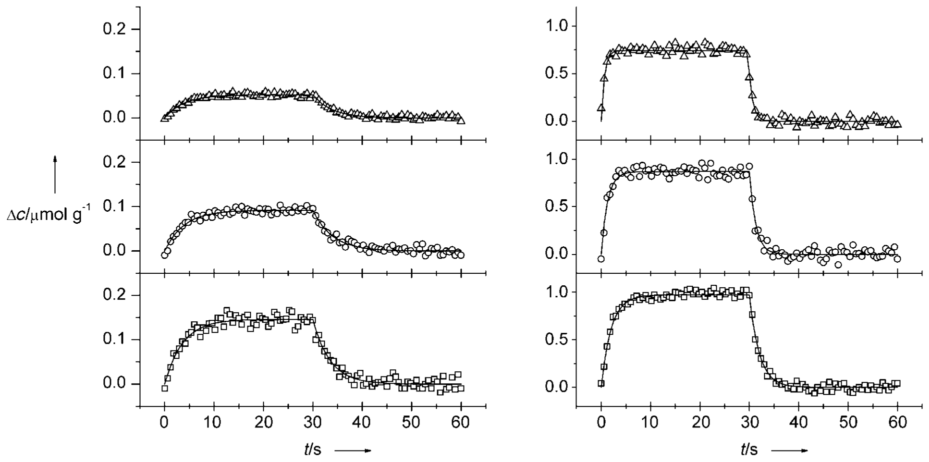

Figure 3. Coverage changes Δc of terminal (left) and bridging hydroxy groups (right) at 403 K on the materials H-ZSM5-p (□), H-ZSM5-1m (○), and H-ZSM5-3m (△) during a periodic volume perturbation around the equilibrium partial pressure of 0.06 mbar.

Table 2: Equilibrium coverage changes, characteristic time constants, and initial sorption rates on terminal and bridging hydroxy groups at 403 K together with the sticking probabilities α for benzene on the series of surface modified H-ZSM5 zeolites.

Sample	SiOH			SiOHAl			$\alpha \times 10^{-7}$
	Δc_{eq} [μmol g^{-1}]	τ [s]	r_{in} [μmol g^{-1} s^{-1}]	Δc_{eq} [μmol g^{-1}]	τ [s]	r_{ini} [μmol g^{-1} s^{-1}]	
H-ZSM5-p	0.145	3.5	0.042	0.978	2.0	0.477	2.10
H-ZSM5-1m	0.096	3.7	0.026	0.907	1.2	0.741	2.48
H-ZSM5-3m	0.060	3.6	0.017	0.722	0.7	1.044	2.96

free SiOH groups (band at 3747 cm^{-1}) in the sequence H-ZSM5-p > H-ZSM5-1m > H-ZSM5-3m, as deduced from the IR spectra of the activated zeolites. In the case of bridging hydroxy groups, the time constant τ decreased continuously from 2.0 to 0.7 s with surface modification, indicating an increasing sorption rate with an increasing amount of SiO_2 deposited during modification. Thus, the sorption rates for the two possible sorption pathways double for the three-fold modified sample compared to the parent sample under identical experimental conditions. This increase appears to be related to the greater sticking probabilities, which also increased by the same factor. Hence, the present data show for the first time that it is possible to increase the sorption rate of benzene by roughening the external surface of the particle by modification. For the nearly rigid and highly symmetric benzene molecule, the roughened surface and the open pore structure allow more entropically favorable orientations of the molecules during collision with the surface, which increases the probability that they are successfully trapped. Benzene colliding with the modified surface appears to be directed to the pore openings. Statistically unfavorable gas-phase orientations, for example with the benzene ring plane distinctly tilted with respect to the zeolite surface, are gradually adjusted during the transport through the overlayer, thus leading to successful trapping and direction of the molecules into the weakly bound physisorbed state. As the formed mesopores have diameters about two times larger than the kinetic diameter of benzene (0.58 nm), additional transport limitations are not generated.

However, this effect would not account for sterically more demanding molecules such as *p*-xylene (length 0.98 nm) with typical dimensions roughly the same size as the large micropores in the SiO_2 layer. Preliminary experiments with such molecules indeed show a retardation of the sorption rate by surface modification. Tailored surface modification increases the sorption rate of molecules that have a kinetic diameter much smaller than the size of the micropores generated in the overlayer. Additional support for this conclusion is given by pressure-step variations of benzene at low coverage. The changes in the coverage of the bridging hydroxy groups with benzene, calculated from the IR intensities, are shown in Figure 4. The initial slopes of the uptake curves directly represent the initial sorption rates and follow the same sequence (H-ZSM5-p < H-ZSM5-1m < H-ZSM5-3m) previously described for the time-resolved experiments with repeated modulation of the pressure in a small interval. The ratios of the SiOHAl sorption rates were 1.8 for H-ZSM5-1m/H-ZSM5-p (sorption is faster for modified sample) and 2.6 for H-ZSM5-3m/H-ZSM5-1m. These ratios are in perfect agreement with the values determined from the uptake rates (summarized in Table 2). Thus, it is well established that the rates of benzene adsorption on the hydroxy groups inside the zeolite pores are strongly enhanced after surface modification with a porous silica overlayer.

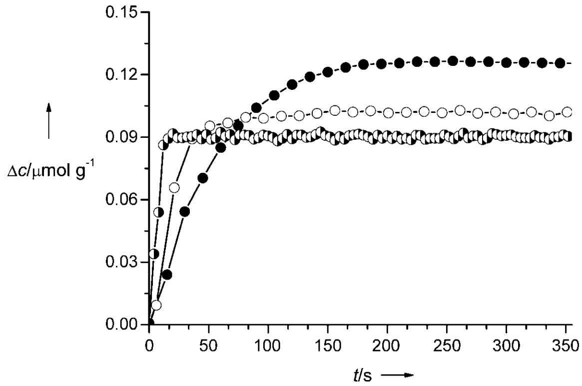

Figure 4. Time-resolved sorption profiles for benzene on SiOHAl sites of H-ZSM5-p (●), H-ZSM5-1m (○), and H-ZSM5-3m (◑) after an initial pressure step from 0 to 0.11 mbar at a temperature of 403 K.

To ensure that the enhancement of the intrapore sorption rates does not result from experimental artifacts or from the blockage of a fraction of the pore volume after modification, sorption isotherms were measured by IR spectroscopy. The uptake of benzene on the SiOHAl groups at the typical pressure difference of the rapid-scan experiment is identical to the uptake calculated from the sorption isotherm at these pressures, thus clearly confirming that all hydroxy groups were accessible (Figure 5). To establish that the higher uptake rates can also be practically implemented for separation processes, transport diffusivities were determined using pressure–frequency response measurements.

The characteristic functions of the frequency response experiment in a temperature range of 343 to 423 K are shown in Figure 6, and the values for the transport diffusivities D_0 are summarized in Table 3. In agreement with the rapid-scan IR spectroscopic measurements, the transport diffusivities increased upon modification, thus revealing faster transport in the modified material. The apparent activation energies of diffusion for parent and modified sample were 23 and 24 kJ mol^{-1}, respectively, and are in the range expected from previous studies.[22,33] The corresponding pre-exponential factors increase significantly from 3.0×10^{-11} to 8.0×10^{-11} m^2 s^{-1} by modification. The equal energies of activation indicate that the surface modification does not increase the energy required for benzene to diffuse into the zeolite. Such an enthalpic barrier leading to higher observed energies of activations for adsorption would have been expected for markedly narrowed pores. In turn, the higher sticking

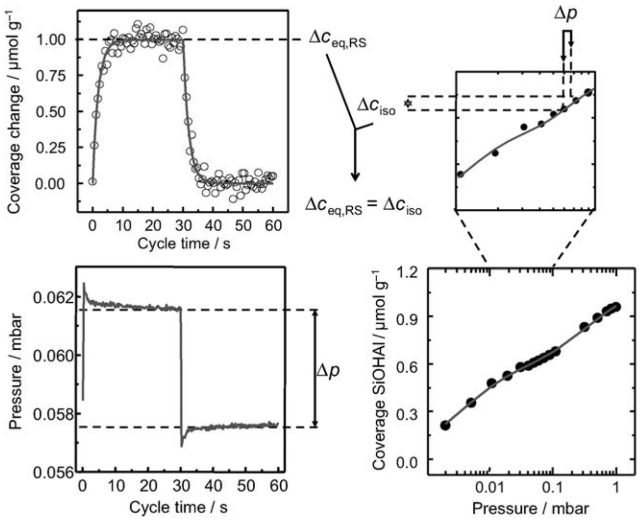

Figure 5. Comparison of the dynamic time-resolved IR spectroscopy measurements (left, top) and the equilibrium sorption isotherms (right) for benzene sorption on the bridging hydroxy groups of unmodified H-ZSM5-p at 403 K. The pressure cycle for the dynamic IR spectroscopy measurements is shown on the bottom left.

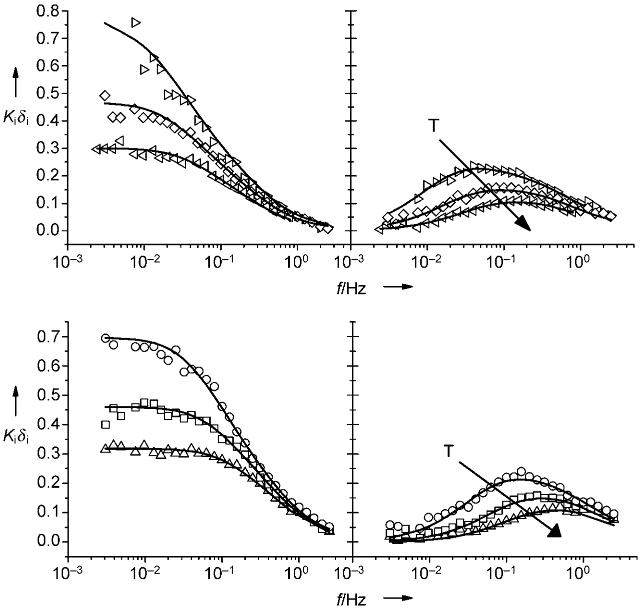

Figure 6. Characteristic in-phase (left) and out-of-phase (right) pressure–frequency response functions $K_i\delta_i$ for benzene on H-ZSM5-p (top) and H-ZSM5-3m (bottom) at 373 (◁, △), 403 (◇, □), and 423 K (▷, ○).

coefficient can be understood by analyzing the elementary steps of the adsorption process.

It has been shown theoretically that the probability for a given molecule to enter a pore dramatically increases as the pore size increases.[34] The amorphous surface layer containing mesopores and large micropores pores will, therefore, allow a larger fraction of molecules to directly adsorb into mesopores, thus enhancing the sticking coefficient. In more general terms, the higher pre-exponential factor is interpreted as being due to the retention of a higher portion of the entropy compared to adsorption on the surface of the parent zeolite (see Figure 1), which has only micropore openings at the outer surface. Note that on the relatively flat surface of the parent zeolite the molecules adsorb into a state similar to a two-dimensional gas, while in the mesoporous surface, a three-dimensional component in the movement of the sorbed particles is retained.

Table 3: Diffusion time constants L^2/D_0, transport diffusivities D_0, and frequency response parameters for equilibrium uptake K at varying temperatures compiled for parent and threefold modified H-ZSM5

	H-ZSM5-p			H-ZSM5-3m		
T [K]	L^2/D_0 [s]	D_0 [m^2 s^{-1}]	K	L^2/D_0 [s]	D_0 [m^2 s^{-1}]	K
343	27.7	9.0×10^{-15}	0.75	9.7	2.6×10^{-14}	0.70
373	14.2	1.8×10^{-14}	0.47	4.7	5.4×10^{-14}	0.46
403	8.9	2.9×10^{-14}	0.30	2.5	1.0×10^{-13}	0.32

The silica overlayer functions as funnel for the sorbing molecules to direct them into the micropores, and it provides for a gradual loss of the entropy instead of the step change found in the parent material (Figure 7). As a direct consequence, the pore diameter of the overlayer is crucial for the successful synthesis of materials with improved sorption properties. The larger the pores, the higher the enhancement should be. On the other hand, we expect to see a gradual reversion of this positive effect as the free rotation of the sorbed molecules in the pores of the overlayer is be hindered with increasing diameter of the sorbed aromatic molecules.

We have shown that new surfaces can be tailored by a hierarchical structure of pores over a microporous material. Such surface modification can be realized by a silica overlayer, which reduces the concentration of terminal free hydroxy groups on the external surface and of nonselective bridging hydroxy groups in the pore-mouth region. It is remarkable that the coverage does not lead to enhanced blockage of a larger portion of the channels and that all acid sites in the zeolite remained accessible after modification. The enhanced sorption rate at sites inside the pores results

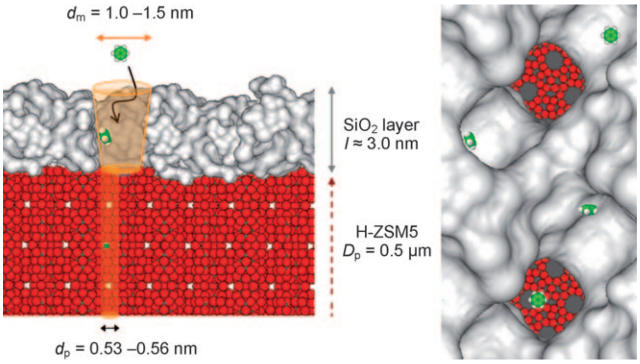

Figure 7. Schematic depiction of H-ZSM5 zeolite crystals shown in cross-section (left), with average diameter $D_p = 0.5$ µm and silica overlayer on the surface with thickness of $l = 2.0$–3.0 nm, and in top view (right). The overlayer, containing large micropores with average diameter d_m around 1.5 nm, functions as a funnel directing the sorbing benzene molecules into the micropores of the zeolite ($d_p = 0.53$–0.56 nm).

primarily from the increase in the sticking probability through the gradual loss of entropy upon collision with the roughened surface and the mesoporous overlayer; this increase is achieved without creating barriers that have to be overcome by energy. This is, however, aided by the effect of the mesopores and large micropores in the overlayer, which lead to a larger concentration of molecules in these pores and as consequence to a larger transport rate to the zeolite micropores. The size of the mesopores needs to be sufficiently large to allow free rotation about the longest axis of the molecule.

Preliminary experiments indicate that the advantage of the overlayer design turns into a disadvantage if this rotation is not possible, leading to a retardation of the sorption of molecules with identical minimum but different maximum diameter. Although unlikely, it cannot be fully excluded, however, that the lower concentration of hydroxy groups at the outer surface also aids the higher uptake rate. The enhancement of the sorption rate into zeolites by chemical modification of the outer surface, as reported herein, highlights a new strategy to enhance separation without an overall retardation of the sorption rates. By tailoring the overlayer pores and maximizing the roughness of the outer surface, it should be possible to synthesize surface-modified materials that enhance the sorption rate of small molecules and at the same time retard the sorption rate for slightly larger ones, even if the two species have identical minimum kinetic diameters.

Experimental Section

Materials: Commercial zeolite H-ZSM5 provided by Süd-Chemie AG with Si/Al = 45:1 (measured by atomic absorption spectroscopy) and an average crystal size of 0.5 μm (evidenced by SEM) was used for the experiments. Concentrations of terminal and bridging hydroxy groups were determined to be 0.27 and 0.21 $\text{mmol}\,\text{g}^{-1}$ by ^{1}H MAS NMR spectroscopy (see Figure S1 in the Supporting Information). Additional ^{27}Al MAS NMR spectroscopy confirmed that there was no change in the concentration of framework aluminum during modification.[35] Postsynthetic surface modification by chemical liquid deposition of tetraethylorthosilicate was performed according to Zheng et al.[35,36] The resulting modified zeolites, denoted H-ZSM5-1m and H-ZSM5-3m, showed concentrations of terminal hydroxy groups of 0.18 and 0.12 $\text{mmol}\,\text{g}^{-1}$ and of bridging hydroxy groups of 0.18 and 0.16 $\text{mmol}\,\text{g}^{-1}$, respectively (determined by ^{1}H MAS NMR; Figures S1 and S2 in the Supporting Information). Spectroscopic-grade benzene (GC standard, > 99.96 %, Sigma–Aldrich) was used without further purification.

Measurements: For IR spectroscopy, the powder samples were pressed into self-supporting wafers (20 $\text{mg}\,\text{cm}^{-2}$) and inserted into a vacuum cell. Activation was performed under vacuum (less than 10^{-7} mbar) at 823 K for 1 h (first heated at the rate of 10 $\text{K}\,\text{min}^{-1}$ and then held at 823 K for 1 h). A periodic volume modulation ($\Delta V = \pm 5\,\%$) was synchronized with the recording of the IR spectra in fast time-resolved rapid-scan mode using a Bruker IFS 66 v/S IR spectrometer. A complete description of the full instrumental setup, including the applied measurement principle, can be found elsewhere.[14,36] TEM images were obtained on a JEOL-2011 electron microscope operated at 200 kV. The transport diffusivities of benzene were measured using the frequency response method on powdered zeolite samples dispersed on several layers of glass wool.[38] Sorbate gases were added with a partial pressure of 0.3 mbar at temperatures between 333 and 423 K, and the system volume was modulated periodically with ± 1 % amplitude in the frequency range of 0.001 to 5 Hz. The pressure response of the system was recorded with a Baratron pressure transducer. A planar sheet model taking into account a Gaussian particle size distribution was used to fit the experimental data. For the mathematical background, we refer to the reviews by Yasuda.[37,38] Nitrogen physisorption was measured using a PMI Automated sorptometer at 77 K after outgassing under vacuum at 473 K for at least 6 h. The apparent surface area was calculated by applying the Brunauer–Emmett–Teller equation to the adsorption isotherms over a relative pressure range from 0.03 to 0.15. The pore volumes were evaluated using the α_s comparative plot[39] with nonporous hydroxylated silica[40] as the reference adsorbent. Pore size distributions were obtained by applying the Barrett–Joyner–Halena (BJH) method[41] on the adsorption branch.

Received: August 6, 2008

Keywords: adsorption · chemical vapor deposition · IR spectroscopy · time-resolved spectroscopy · zeolites

[1] G. Kokotailo, S. Lawton, D. Olson, W. Meier, *Nature* **1978**, *272*, 437.
[2] A. Corma, *Chem. Rev.* **1995**, *95*, 559.
[3] J. Weitkamp, *Solid State Ionics* **2000**, *131*, 175.
[4] P. R. Pujadó, J. A. Rabo, G. J. Antos, S. A. Gembicki, *Catal. Today* **1992**, *13*, 113.
[5] P. B. Weisz, *Pure Appl. Chem.* **1980**, *58*, 841.
[6] I. I. Ivanova, A. Corma in *Zeolites: A Refined Tool For Designing Catalytic Sites*, *Vol. 97*, Elsevier Science, Amsterdam, **1995**, p. 27.
[7] X. D. Sun, Q. X. Wang, L. Y. Xu, S. L. Liu, *Catal. Lett.* **2004**, *94*, 75.
[8] T.-C. Tsai, S.-B. Liu, I. Wang, *Appl. Catal. A* **1999**, *181*, 355.
[9] G. Mirth, J. A. Lercher, *J. Catal.* **1994**, *147*, 199.
[10] S. M. Csicsery, *Pure Appl. Chem.* **1986**, *58*, 841.
[11] E. Klemm, G. Emig, *Chem. Eng. Sci.* **1997**, *52*, 4329.
[12] E. Klemm, J. G. Wang, G. Emig, *Chem. Eng. Sci.* **1997**, *52*, 3173.
[13] J. Weitkamp, A. Raichle, Y. Traa, M. Rupp, F. Fuder, *Chem. Commun.* **2000**, 1133.
[14] A. Jentys, H. Tanaka, J. A. Lercher, *J. Phys. Chem. B* **2005**, *109*, 2254.
[15] P. B. Weisz, V. Frilette, *J. Phys. Chem.* **1960**, *64*.
[16] B. Smit, T. L. M. Maesen, *Nature* **2008**, *451*, 671.
[17] A. Jentys, H. Tanaka, J. A. Lercher, *Stud. Surf. Sci. Catal.* **2004**, *154*, 2041.
[18] F. R. Ribeiro, F. Alvarez, C. Henriques, F. Lemos, J. M. Lopes, M. F. Ribeiro, *J. Mol. Catal. A* **1995**, *96*, 245.
[19] G. Sastre, N. Raj, C. R. A. Catlow, R. Roque-Malherbe, A. Corma, *J. Phys. Chem. B* **1998**, *102*, 3198.
[20] U. Schemmert, J. Kärger, J. Weitkamp, *Microporous Mesoporous Mater.* **1999**, *32*, 101.
[21] R. Q. Snurr, A. T. Bell, D. N. Theodorou, *J. Phys. Chem.* **1993**, *97*, 13742.
[22] L. Song, Z.-L. Sun, L. V. C. Rees, *Microporous Mesoporous Mater.* **2002**, *55*, 31.
[23] S. Brandani, M. Jama, D. M. Ruthven, *Ind. Eng. Chem. Res.* **2000**, *39*, 821.
[24] L. V. C. Rees, D. M. Shen, *Characterization of Porous Solids III*, *Vol. 87*, Elsevier Science, Amsterdam, **1994**, pp. 563.
[25] S. I. Reshetnikov, S. B. Ilyin, A. A. Ivanov, A. S. Kharitonov, *Reac. Kin. Catal. Lett.* **2004**, *83*, 157.
[26] H. G. Karge, *Abstr. Pap. Am. Chem. Soc.* **1993**, *205*, 143.
[27] J. Kärger, *Adsorption* **2003**, *9*, 29.
[28] C. Förste, A. Germanus, J. Karger, H. Pfeifer, J. Caro, W. Pilz, A. Zikanova, *J. Chem. Soc. Faraday Trans. 1* **1987**, *83*, 2301.

[29] Y. Fu, F. Ye, W. G. Sanders, M. M. Collinson, D. A. Higgins, *J. Phys. Chem. B* **2006**, *110*, 9164.
[30] S. J. Reitmeier, R. R. Mukti, A. Jentys, J. A. Lercher, *J. Phys. Chem. C* **2008**, *112*, 2538.
[31] Y. S. Bhat, J. Das, K. V. Rao, A. B. Halgeri, *J. Catal.* **1996**, *159*, 368.
[32] M. Schenk, S. Calero, T. M. L. Maesen, T. J. H. Vlugt, L. L. van Benthem, B. Schnell, B. Smit, *J. Catal.* **2003**, *214*, 88.
[33] L. J. Song, L. V. C. Rees, *Microporous Mesoporous Mater.* **2000**, *35*, 301.
[34] A. I. Skoulidas, D. S. Sholl, *J. Chem. Phys.* **2000**, *113*, 4379.
[35] S. Zheng, H. R. Heydenrych, A. Jentys, J. A. Lercher, *J. Phys. Chem. B* **2002**, *106*, 9552.
[36] S. R. Zheng, H. Tanaka, A. Jentys, J. A. Lercher, *J. Phys. Chem. B* **2004**, *108*, 1337.
[37] Y. Yasuda, *Heterog. Chem. Rev.* **1994**, *1*, 103.
[38] Y. Yasuda, *Zeolites and Related Microporous Materials: State of the Art*, *Vol. 84*, Elsevier Science, Amsterdam, **1994**, p. 1331.
[39] M. Kruk, M. Jaroniec, J. Choma, *Carbon* **1998**, *36*, 1447.
[40] S. J. Gregg, *Adsorption Surface Area and Porosity*, 2nd ed., Academic Press, New York, **1982**.
[41] S. Brunauer, P. H. Emmett, E. Teller, *J. Am. Chem. Soc.* **1938**, *60*, 309.